Apoptotic Cleavage of Cytoplasmic Dynein Intermediate Chain and p150^{Glued} Stops Dynein-dependent Membrane Motility

Jon D. Lane, Maïlys A.S. Vergnolle, Philip G. Woodman, and Victoria J. Allan

School of Biological Sciences, University of Manchester, Manchester M13 9PT, United Kingdom

Abstract. Cytoplasmic dynein is the major minus end–directed microtubule motor in animal cells, and associates with many of its cargoes in conjunction with the dynactin complex. Interaction between cytoplasmic dynein and dynactin is mediated by the binding of cytoplasmic dynein intermediate chains (CD-IC) to the dynactin subunit, p150^{Glued}. We have found that both CD-IC and p150^{Glued} are cleaved by caspases during apoptosis in cultured mammalian cells and in *Xenopus* egg extracts. *Xenopus* CD-IC is rapidly cleaved at a conserved aspartic acid residue adjacent to its NH_2-terminal p150^{Glued} binding domain, resulting in loss of the otherwise intact cytoplasmic dynein complex from membranes. Cleavage of CD-IC and p150^{Glued} in apoptotic *Xenopus* egg extracts causes the cessation of cytoplasmic dynein–driven endoplasmic reticulum movement. Motility of apoptotic membranes is restored by recruitment of intact cytoplasmic dynein and dynactin from control cytosol, or from apoptotic cytosol supplemented with purified cytoplasmic dynein–dynactin, demonstrating the dynamic nature of the association of cytoplasmic dynein and dynactin with their membrane cargo.

Key words: microtubule • motor • apoptosis • trafficking • caspase

Introduction

Apoptosis, or programmed cell death, is accompanied by the activation of a family of apoptosis-specific cysteine proteases called caspases (Cohen, 1997). Both the signaling pathways that mediate caspase activation, and the substrates for caspases, are highly conserved. The so-called execution phase of apoptosis involves a characteristic series of morphological changes that in many cases are directly coupled to caspase-dependent cleavage of key substrates. These events ultimately lead to the recognition and engulfment of dying cells by their neighbors. The nature of the phagocytic signal generated by the apoptotic cell is not known, but is likely to be complex. This is perhaps best illustrated by the finding that "professional" and "nonprofessional" phagocytic cells clear apoptotic cells at different rates, with the latter recognizing apoptotic cells only after the execution phase has run its full course (Parnaik et al., 2000).

The exposure of phosphatidyl serine on the surface of apoptotic cells is thought to be a key phagocytic signal (Martin et al., 1995; Fadok et al., 2000; Hamon et al., 2000), but other markers are clearly important (Savill et al., 1990; Ren et al., 1995; Platt et al., 1996; Devitt et al., 1998). Indeed, since such widely recognized phagocytic signals must be generic, it is probable that general alterations in the protein composition of the plasma membrane, or in the glycosylation of proteins or lipids, are also involved. Such changes could be brought about by altering the specificity or efficiency of membrane traffic pathways. In support of this hypothesis, there is evidence that both the secretory and endocytic pathways are affected in apoptotic cells. There are profound changes in membrane structure (Wyllie et al., 1980), including fragmentation of the Golgi complex (Mancini et al., 2000) and inhibition of the secretory pathway (Whyte et al., 1993). In addition, homotypic endosome fusion is inhibited in apoptotic cell extracts via the caspase 3–dependent cleavage of Rabaptin 5 (Cosulich et al., 1997; Swanton et al., 1999a).

The secretory and endocytic pathways rely in numerous ways on the function of cytoplasmic dynein and its regulator dynactin. They are required for ER-to-Golgi region traffic (Presley et al., 1997), for maintaining Golgi apparatus organization and position (Burkhardt et al., 1997; Harada et al., 1998; Quintyne et al., 1999; Roghi and Allan, 1999), and for moving endocytic organelles and facilitating traffic between them (Blocker et al., 1997; Harada et al., 1998; Valetti et al., 1999). The ER itself is a cargo for cytoplasmic dynein in extracts of *Xenopus* eggs and early embryos (Allan, 1995; Lane and Allan, 1999). In addition to these roles in trafficking, cytoplasmic dynein, and dynactin are also needed for maintaining microtubule organization in interphase, as well as for correct spindle

P.G. Woodman and V.J. Allan contributed equally to this work.

Address correspondence to Victoria J. Allan, School of Biological Sciences, University of Manchester, 2.205 Stopford Building, Oxford Road, Manchester M13 9PT, UK. Tel.: (44) 161-275-5646. Fax: (44) 161-275-5082. E-mail: viki.allan@man.ac.uk

assembly, positioning, and chromosome attachment during cell division (for review see Karki and Holzbaur, 1999).

The central importance of cytoplasmic dynein in maintaining cellular architecture makes it an attractive target for inactivation during apoptosis. Cytoplasmic dynein is a large molecule (~1.2 MDa) which consists of two heavy chains (CD-HC),[1] two or three intermediate chains (CD-IC), four light intermediate chains (CD-LIC), and a variety of light chains (for review see Susalka et al., 2000). More than one gene exists for the heavy, intermediate, and light intermediate chains, and in addition, the CD-ICs and the CD-LICs undergo tissue-specific alternate splicing (Susalka et al., 2000). Whether different subsets of these chains associate to give cytoplasmic dynein molecules with distinct function is not clear, but seems likely (Susalka et al., 2000).

Cytoplasmic dynein function generally requires dynactin, first identified as an activator of cytoplasmic dynein–driven vesicle movement (Gill et al., 1991). Dynactin also consists of multiple subunits, including two p150^{Glued} chains which extend out from a short filament of actin-related protein 1 which associates with a variety of other subunits, including several dynamitin molecules (Schafer et al., 1994; Quintyne et al., 1999). Genetic and biochemical studies have confirmed that the two complexes must interact for virtually all cytoplasmic dynein functions (for review see Allan, 1996; Schroer, 1996; Karki and Holzbaur, 1999). Dynactin is thought to link cytoplasmic dynein to its cargoes (for review see Allan, 1996; Schroer, 1996; Karki and Holzbaur, 1999) and to enhance cytoplasmic dynein's processivity (King and Schroer, 1999). How dynactin attaches to cargoes is not clear, but it might bind directly to membrane lipids, or interact with proteins such as beta spectrin on the Golgi apparatus or ZW10 on the kinetochore (Karki and Holzbaur, 1999; Muresan et al., 2001). Cytoplasmic dynein then binds to dynactin via an interaction between p150^{Glued} and the NH_2-terminal domain of CD-IC (Karki and Holzbaur, 1995; Vaughan and Vallee, 1995).

A convenient system for studying cytoplasmic dynein function during apoptosis is provided by *Xenopus* egg extracts, which support active cytoplasmic dynein–driven ER movement (Allan, 1995; Niclas et al., 1996; Lane and Allan, 1999) and can readily be made apoptotic (Kluck et al., 1997). Here, we show that CD-IC and p150^{Glued} are cleaved by caspases both in apoptotic egg extracts and during apoptosis in vivo. The implications of these cleavage events for cytoplasmic dynein–dynactin function are described.

Materials and Methods

Chemicals and Antibodies

Unless otherwise stated, chemicals were obtained from Sigma-Aldrich. Stock solutions were stored at −20°C: anisomycin (5 mg/ml in DMSO), etoposide (50 mM in DMSO), and caspase inhibitors (Ac-DEVD.CHO at 100 μM and zVAD.FMK at 50 μM, both in DMSO; Calbiochem-Novabiochem). Protease inhibitors (leupeptin, chymostatin, pepstatin, and aprotinin) were used at 10 μg/ml final concentration.

For immunoblotting, we used the following monoclonal antibodies: anti–CD-IC (70.1, Sigma-Aldrich; 1618, Chemicon International), anti-p150^{Glued} (Transduction Labs), antifodrin (ICN Biomedicals), antitubulin (B-5-1-2), antiribophorin (CEL5C, from Birgit Lane, University of Dundee, Dundee, UK), antikinesin II (K 2.4, from John Scholey, University of California at Davis, Davis, CA), and anti-p50 dynamitin (from Richard Vallee, University of Massachusetts, Worcester, MA); and the following polyclonal antibodies: anti-rat CD-IC (from Richard Vallee; Vaughan and Vallee, 1995), anti-*Xenopus* CD-LIC (Addinall et al., 2001), anti–CD-IC NH_2 terminus (*Xenopus*-specific; Lane and Allan, 1999), anti-*Xenopus* CD-IC peptide antibody (raised and affinity purified against the sequence NRSNKRTPVQRTPLS; underlined in Fig. 3), anti–poly-ADP-ribose polymerase (PARP; Calbiochem), antikinesin heavy chain (KHC; from Ron Vale, University of California at San Francisco, San Francisco, CA), anti–β-COP (D1; from Thomas Kreis, University of Geneva, Geneva, Switzerland), and anti–Arp-1 (centractin; from David Meyer, University of California at Los Angeles, Los Angeles, CA). Secondary antibodies (conjugated to alkaline phosphatase or horse radish peroxidase) were from Jackson ImmunoResearch Laboratories.

Extract Preparation and Analysis

HL60 cells were grown in RPMI 1640 plus 10% foetal bovine serum and penicillin/streptomycin. To analyze apoptosis in vivo, cells were treated with 5 μg/ml anisomycin or 50 μM etoposide, with or without a 30 min preincubation with 50 μM zVAD-FMK. Cells were washed three times in PBS, then broken by passing 20 times through a cell cracker (Balch et al., 1984) in acetate/sucrose buffer (100 mM K-acetate, 3 mM Mg-acetate, 5 mM EGTA, 10 mM Hepes, pH 7.4, 150 mM sucrose) containing protease inhibitors. Postnuclear supernatants were prepared and stored at −80°C.

Interphase *Xenopus* egg extracts were prepared as described (Murray, 1991). Apoptotic or control extracts were generated by the addition of cytochrome *c* (to 10 μM) ± the caspase inhibitor, Ac-DEVD-CHO (2 μM), followed by incubation for 8 h at 25°C. Cytosol and membranes were prepared from control and apoptotic extracts, and membranes were further purified by flotation (Lane and Allan, 1999). For biochemical analysis of rebinding to membrane, isolated membranes (10 μl 5 mg/ml protein) were incubated in 90 μl control or apoptotic cytosol at 25°C for 60 min. The mixture was then centrifuged in a rotor (TLA100; Beckman Coulter) for 15 min at 40,000 g_{av} at 4°C through a 150-μl cushion of 0.75 M sucrose in acetate buffer. The pelleted membranes were analyzed by immunoblotting.

Biochemical Analysis of Motor Complexes

Cytoplasmic dynein and dynactin were isolated from 400 μl control or apoptotic cytosols by microtubule affinity and sucrose density gradient centrifugation as described (Niclas et al., 1996). 50-μl fractions were collected and run on 4–15% gradient acrylamide gels then analyzed by silver staining and immunoblotting. Immunoprecipitation experiments were performed as described (Roghi and Allan, 1999). In brief, 20 μl of control or apoptotic egg cytosol was diluted to 500 μl in immunoprecipitation buffer then incubated with protein G Sepharose beads (Zymed Laboratories) prebound with anti–CD-IC (1618) or anti–CD-LIC antibodies.

Motility Assays and Data Collection

Motility assays were performed using video-enhanced differential interference contrast (VE-DIC) microscopy using a light microscope (BX60; Olympus) (Allan, 1998). To compensate for differences in microtubule assembly between control and apoptotic cytosols, a uniform field of stable microtubules was assembled. Flow cells were perfused with diluted control egg cytosol (1:20 in acetate/sucrose) for 5 min. After two washes with 10 μl acetate/sucrose, taxol-stabilized microtubule seeds (Allan and Vale, 1991) were added. After 10 min, soluble tubulin (5 mg/ml) plus 1 mM GTP was introduced, and microtubules were allowed to grow for 15 min. Microtubules were stabilized by flowing through 20 μM taxol in acetate/sucrose, washed once with acetate/sucrose, and then a mix of cytosol and membranes was added. Over time, ER networks assemble on the coverslip surface in a cytoplasmic dynein–dependent fashion. Network formation was quantitated after 45 min by counting the number of three way junctions in 20 random fields, which correlate directly with the quantity of cytoplasmic dynein–based movement (Allan, 1995). Motility experiments were carried out in the presence of 2 μM Ac-DEVD-CHO to prevent further caspase action.

PCR and Cloning of Xenopus CD-IC

The first 288 bases of *Xenopus* CD-IC were obtained from a frog oocyte cDNA library (Nicolás et al., 1997) by degenerate PCR using the follow-

[1]*Abbreviations used in this paper:* CD-HC, cytoplasmic dynein heavy chain; CD-IC, CD intermediate chain; CD-LIC, CD light intermediate chain; KHC, kinesin heavy chain; PARP, poly-ADP-ribose polymerase; VE-DIC, video-enhanced differential interference contrast.

ing primers: forward, GGGGATCCATGTC(I)GA(CT)AA(AG)AG-(CT)GA(I)(CT)T(I)AA; reverse, GGAATTC(AG)TC(CT)TG(AG)C-T(I)CC(I)GC(AG)CT(I)GG. The PCR product was cloned into pBluescript (pBSIIsk+; Stratagene), and was used to prepare a probe to screen the oocyte cDNA library to obtain a full-length *Xenopus* CD-IC clone. A single clone was isolated, the sequence of which was most similar to CD-IC2B (these sequence data are available from EMBL/GenBank/DDBJ under accession nos. AF319780 and AF319781). The clone lacked the first 90 bases from the 5′ end, so to obtain a full-length construct it was joined to the original PCR product using a conserved NsiI site within the overlapping region. Site-directed mutagenesis was performed using the QuikChange kit (Stratagene). All mutations were confirmed by sequencing.

In Vitro Transcription/Translation

The full-length *Xenopus* CD-IC construct was subcloned into the expression vector, pCDNA3.1 (Invitrogen). [^{35}S]methionine-labeled protein was produced using a coupled transcription/translation kit (Promega). Translations were analyzed by autoradiography. Translated *Xenopus* CD-IC appeared as several 60–85-kD bands (data not shown), which were probably derived from random initiation events, so CD-IC was routinely immunoprecipitated using an NH_2-terminal anti–CD-IC antibody (1618). The immunecomplex was then used in caspase cleavage assays. Recombinant PARP and caspase 2 were prepared as described (Swanton et al., 1999b).

Caspase Cleavage Assays

Assays using recombinant caspases 2, 3, and 7 (Alexis Biochemicals; and from Don Nicholson and Sophie Roy [Merk Frosst Centre for Therapeutic Research, Quebec, Canada]) were performed in caspase buffer (for caspases 3 and 7; 50 mM Hepes-KOH, pH 7.0, 2 mM EGTA, 0.1% Chaps, 10% sucrose, 5 mM DTT; for caspase 2, 50 mM Na-citrate, pH 5.5 replaced the Hepes-KOH). Fractions enriched in native *Xenopus* or pig brain cytoplasmic dynein–dynactin were incubated with caspases for 3 h at 37°C and analyzed by silver staining and immunoblotting.

Cleavage of in vitro–translated, immunoprecipitated, [^{35}S]methionine-labeled *Xenopus* CD-IC was carried out either by incubating beads in control or apoptotic egg cytosol for 6 h at 25°C, or by incubating beads in the presence of recombinant caspases for 2 h at 30°C. Radiolabeled products were detected by autoradiography. For some experiments the caspase 3 and 7 inhibitor, Casputin™ (Biomol Research Laboratories, Inc.; 80 μg/ml final) was included.

Results

CD-IC and p150^{Glued} Are Targets for Caspases during Apoptosis

To investigate whether the inactivation of microtuble motors might contribute to the changes in cell morphology associated with apoptosis, we assessed the stability of a variety of molecules after activation of caspases in intact cells. We used a number of cell lines (including human HL60, jurkat and A431, and rat NRK) treated with a selection of drugs (anisomycin, etoposide, staurosporine, or camptothecin). Most molecules tested (namely KHC, kinesin II, p50 dynamitin, β-COP, and tubulin [Fig. 1 A]) were not altered during apoptosis. However, loss of immunoreactivity of both CD-IC and the p150^{Glued} component of the dynactin complex was seen in apoptotic cells (Fig. 1, A and B). In HL60 cells undergoing apoptosis in response to 5 μg/ml anisomycin or 50 μM etoposide (Fig. 1 B), CD-IC rapidly became undetectable at about the same rate that the characterized caspase substrate PARP was cleaved. This suggests that CD-IC may be an early target for caspases. The reduction in p150^{Glued} signal was more gradual, mirroring the loss of full-length fodrin immunoreactivity (Fig. 1 B). In each case, loss of immunoreactivity was greatly reduced by the cell permeable caspase inhibitor zVAD-FMK.

To study how caspase-dependent cleavage of CD-IC and p150^{Glued} affect the function of the cytoplasmic dynein–dynactin complex, we examined the cleavage of both proteins in vitro using *Xenopus* egg extracts, since they are well-suited for studying motor proteins (Allan and Vale, 1991) and apoptosis (Newmeyer et al., 1994). Apoptosis can be triggered in cell-free extracts by the addition of cytochrome *c* (Liu et al., 1996; Kluck et al., 1997), whereupon effector caspases are activated (e.g., Swanton et al., 1999b). A clear reduction in recognition of CD-IC by NH_2-terminal monoclonal antibodies was seen upon addition of cytochrome *c* to *Xenopus* egg extracts, but no cleavage products were detected (Fig. 1 C). This loss of signal occurred over a similar time scale to the cleavage of other caspase substrates in *Xenopus* extracts (Newmeyer et al., 1994; Cosulich et al., 1996) and was prevented by the caspase inhibitor Ac-DEVD-CHO (Fig. 1 C). In contrast, the monoclonal antibody to p150^{Glued} detected a cleavage product in apoptotic egg extracts, ~10–20 kD smaller than the native molecule (Fig. 1 C); no such product was seen in HL60 extracts, although the p150^{Glued} antibody reactivity was lost with time (Fig. 1, A and B). We do not yet know why the pattern of p150^{Glued} cleavage differs in these two systems.

CD-IC Is Cleaved within Its NH_2-terminal p150^{Glued} Binding Domain

To drive the movement of a variety of cargoes towards the minus ends of microtubules, cytoplasmic dynein interacts with dynactin through binding of the NH_2 terminus of CD-IC to p150^{Glued} (Fig. 2, A and B; Karki and Holzbaur, 1995; Vaughan and Vallee, 1995). This region of CD-IC is recognized by both monoclonal antibodies 70.1 and 1618 (data not shown). Since neither antibody recognized cleavage products in apoptotic cells and extracts (Fig. 1), this suggested that caspase-dependent cleavage occurs within this region. To test this hypothesis, we used a polyclonal antiserum raised against full-length rat CD-IC (Vaughan and Vallee, 1995), and a peptide antibody raised against a sequence towards the COOH-terminus of CD-IC (see Materials and Methods; Fig. 3). In immunoblots of apoptotic *Xenopus* egg extracts, these antibodies revealed a cleavage product ~12 kD smaller than the molecular mass of the full-length molecule (Fig. 2 C). These data suggest that CD-IC is cleaved by caspases within its NH_2-terminal p150^{Glued} binding domain.

Comparison of multiple CD-IC sequences revealed several conserved aspartic acids towards the NH_2 terminus of the molecule (Fig. 3). To identify the caspase cleavage site, we used site-directed mutagenesis to alter these aspartic acids to alanine, and examined the cleavage of in vitro–translated, [^{35}S]methionine-labeled protein when added to apoptotic egg cytosol. Two cleaved products were generated from in vitro–translated wild-type *Xenopus* CD-IC (Fig. 4 A): one at ~74 kD (C_1) and one at ~66 kD (C_2). C_1 matches the size of the product seen in immunoblots of apoptotic egg extracts using the polyclonal anti–CD-IC (Fig. 2 C), whereas we have never observed a band of the size of C_2, perhaps because the C_2 cleavage site is inaccessible when CD-IC is in the native cytoplasmic dynein complex. Mutating the putative site DSGD^{99}G (D→A) resulted in the loss of the upper cleavage product (C_1) (Fig. 4 A).

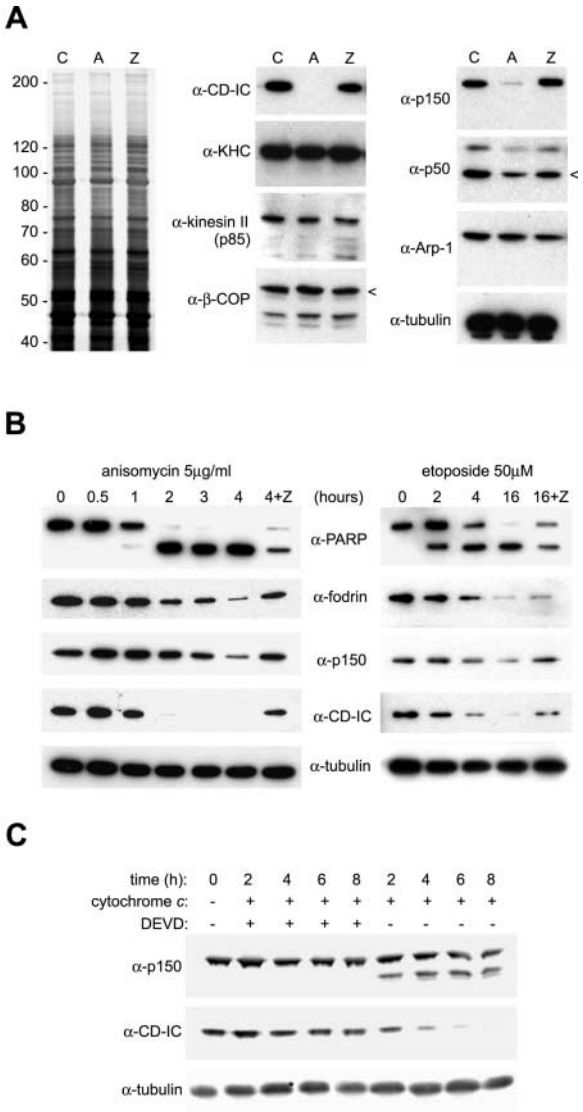

Figure 1. CD-IC and p150^{Glued} are cleaved during apoptosis. (A) Cytosols were made from untreated human HL60 cells (C), cells treated with anisomycin (A; 5 μg/ml) for 4 h, and cells treated with anisomycin and the cell-permeable capsase inhibitor zVAD.FMK (Z). Equal amounts of protein were analyzed by silver staining (left) and immunoblotting. The positions of full-length β-COP and p50 are shown (<). (B) HL60 cells were treated with 5 μg/ml anisomycin or 50 μM etoposide. Cell extracts prepared at the indicated times were immunoblotted using the antibodies shown. Samples treated for the maximum times with each agent in the presence of zVAD.FMK are also shown (Z). (C) A *Xenopus* egg extract was incubated with 10 μM cytochrome *c* ± the caspase inhibitor Ac-DEVD-CHO for the times indicated. Extracts were then analyzed by immunoblotting. In all panels, the anti–CD-IC antibody used was 70.1.

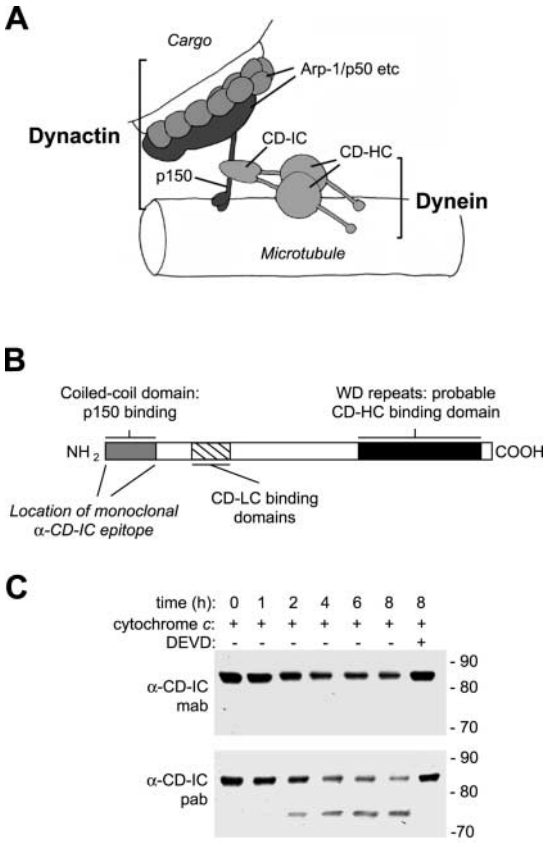

Figure 2. Cleavage of CD-IC takes place within its NH_2-terminal p150^{Glued} binding region. (A) Schematic diagram of cytoplasmic dynein and dynactin, showing the interaction between the NH_2 terminus of CD-IC and p150^{Glued}. (B) Representation of CD-IC showing the regions that interact with other components of the cytoplasmic dynein and dynactin complexes. (C) Immunoblot of a *Xenopus* egg extract that had been treated for the times indicated (in hours) with cytochrome *c* ± Ac-DEVD-CHO using monoclonal (70.1) and polyclonal antibodies to CD-IC. The positions of molecular weight markers are also shown.

None of the other mutations altered the pattern of cleavage of *Xenopus* CD-IC (data not shown).

Since DSGD^{99}G fits with consensus sites for caspase 3 (DXXD motif), we tested the effects of the selective caspase 3 and 7 inhibitor, Casputin™. This inhibitor prevented cleavage of in vitro–translated wild-type CD-IC to C_1 (Fig. 4 A), suggesting that this product is generated by caspase 3 or caspase 7 in apoptotic egg extracts. We then tested the ability of recombinant caspases 2, 3, and 7 to cleave in vitro–translated, immunoprecipitated CD-IC (Fig. 4, B–D). These caspases were shown to be active by incubating them with known substrates. All three caspases cleaved CD-IC to generate C_1, to varying degrees, with caspase 3 being most effective. From these data, caspase 3 is the best candidate for cleaving CD-IC at DSGD^{99}G.

To confirm that CD-IC within native cytoplasmic dynein could be cleaved by caspase 3, we carried out in vitro cleavage assays using recombinant caspases 2 and 3, and cytoplasmic dynein–dynactin fractions prepared from *Xenopus* eggs (Fig. 4 E). Using immunoblotting, we demonstrated that endogenous *Xenopus* CD-IC was degraded in vitro by caspase 3, but much less so by caspase 2 (Fig. 4 E). Caspase 3, but not 2, also cleaved some of the p150^{Glued} present within the same fraction (Fig. 4 E). The inclusion of Ac-DEVD-CHO in these assays prevented caspase-mediated CD-IC and p150^{Glued} cleavage. Identical results were obtained using pig brain cytoplasmic dynein–dynactin (data not shown).

```
Rn CD-IC1A   1   MSDKSDLKAELERKK QRLAQIREEKKRKEE ERKKKEADMQQ-KKE PVPDDSDLDRKRRET  59
Rn CD-IC2A   1   MSDKSELKAELERKK QRLAQIREEKKRKEE ERKKKETDQKKEAAV SVQEESDLEKKRREA  60
Rn CD-IC2B   1   MSDKSELKAELERKK QRLAQIR-EEKKRKE EERKKKETDQKEAAV SVQEESDLEKKRREA  59
Rn CD-IC2C   1   MSDKSELKAELERKK QRLAQ-REEKKRKEE ERKKKETDQKKEAAV SVQEESDLEKKRREA  59
Xl CD-IC     1   MSDKSELKAELERKK QRLAQIREEKKRKEE EKKKKETDQKKD-AV PTQEESDLEKKRREA  59

Rn CD-IC1A  60   EALLQSIGISPEPPL VQPLHFLTWDTCYFH YLVPTPMSPSSKSVS TPSEAGSQD--DLG- 116
Rn CD-IC2A  61   EALLQSMGLTTDSPI V-----------FSE HWVPPPMSPSSKSVS TPSEAGSQDSGDGA- 108
Rn CD-IC2B  60   EALLQSMGLTTDSPI ---------------- --VPPPMSPSSKSVS TPSEAGSQDSGDA-- 100
Rn CD-IC2C  60   EALLQSMGLTTDSPI ---------------- --VPPPMP-SSKSVS TPSEAGSQDSGDGA- 100
Xl CD-IC    60   DALLQSMGITSEPP- ---------------- -MVPPPTSPSSKSVS TPSEAGSQDSGDGAG 102

Rn CD-IC1A 117 -------PLTRTLQW DTDPSVLQLQSDSEL GRRLNKLGVSKVTQV DFLPREVVSYSKETQ 169
Rn CD-IC2A 109 -------VGSRTLHW DTDPSALQLHSDSDL GRGPIKLGMAKITQV DFPPREIVTYTKETQ 161
Rn CD-IC2B 101 -------VGSRTLHW DTDPSALQLHSDSDL GRGPIKLGMAKITQV DFPPREIVTYTKETQ 154
Rn CD-IC2C 101 -------VGSR---- ---------------- -RGPIKLGMAKITQV DFPPREIVTYTKETQ 134
Xl CD-IC   104 GASARTAVTTKTLHW DTDPSVLQLHSDSDM GRGPMKLGMSKVTQV DFAPRETVSYTKETQ 162

Xl CD-IC   165 TPILAQNNEGDEDEE ETVAPKAVTVQEEDK PEKKEENTEAPPHEL TEEEKQQILHSEEFV 225
           226 SFFDHSTRILERALS EQINIFFDYSGRDLE EKEGEIQAGAKLSFN RQFFDERWSKHRVVS 286
           287 CLDWSSQYPELLVAS YNNNEDAPHEPDGVA LVWNMKYKKTTPEYV FHCQSAVMSAAFARF 347
           348 HPNLVVGGTYSGQIV LWDNRSNKRTPVQRT PLSAAAHTHPVYCVN VVGTQNAHNLISIST 408
           409 DGKICSWSLDMLSQP QDSMELVHKQSKAVA VTCMSFPVGDVNNFV VGSEEGSVYTACRHG 469
           470 SKAGISEMFEGHQGP ITGIHCHSAVGAVDF SHLFITSSFDWTVKL WTTKNNKPLYSFEDN 530
           531 SDYVYDVMWSPTHPA LFACVDGVGRLDLWN LNNDTEVPTASITVD GNPALNRVRWTHSGR 691
           692 EIAVGNSEGEIFIYD VGEQTAVPRSDEWTR FARTLAEINANRADA EEEAANRIPG     760
```

Figure 3. Amino acid sequence of *Xenopus laevis* (Xl) CD-IC aligned with the NH_2 terminus of rat (Rn) CD-IC1, 2A, 2B, and 2C. The locations of several potential caspase cleavage motifs are highlighted. In each of these, the crucial aspartic acid residue at position P_1 ($P_4P_3P_2P_1$) of *Xenopus* CD-IC was altered by site-directed mutagenesis. The peptide sequence used for polyclonal antibody production is underlined.

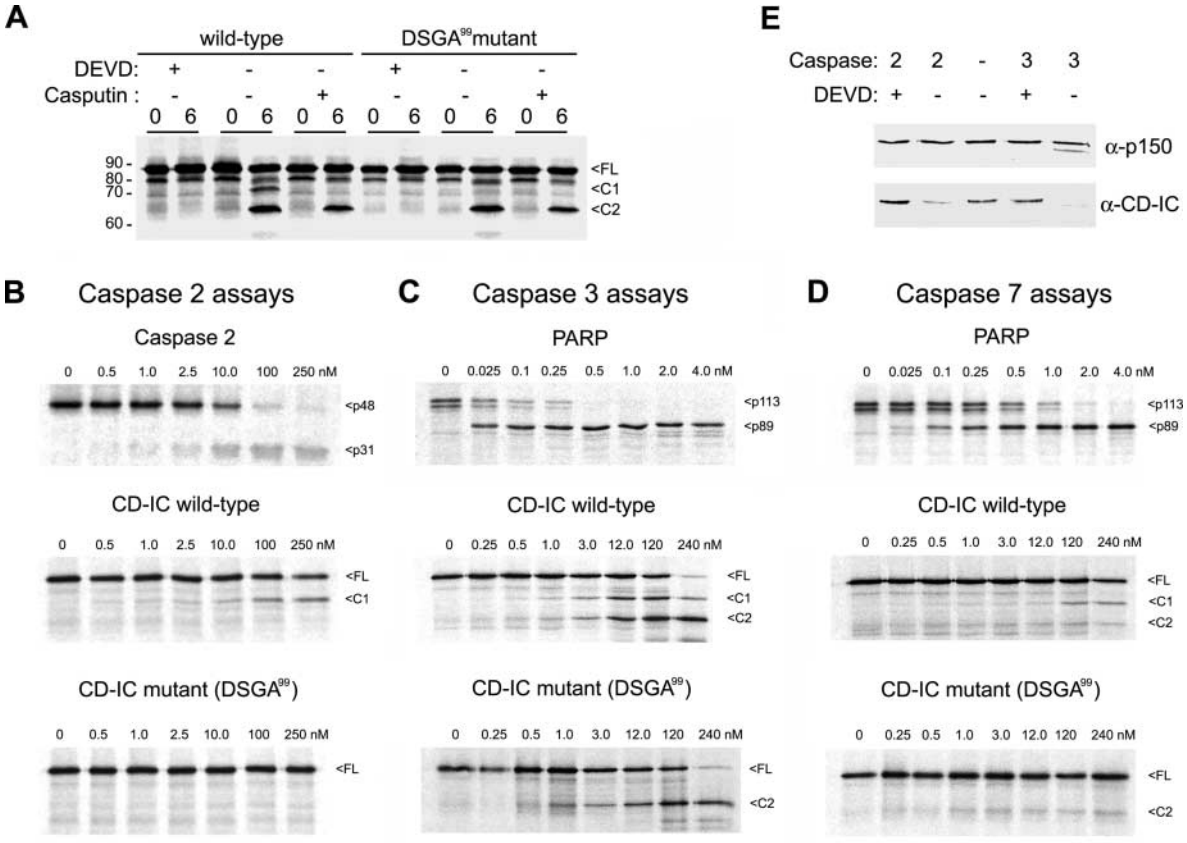

Figure 4. Cleavage of *Xenopus* CD-IC in vitro occurs at $DSGD^{99}$ and at another, unidentified site. (A) Immunoprecipitated [^{35}S]methionine-labeled wild-type or mutated ($DSGA^{99}$) CD-IC was incubated in apoptotic *Xenopus* egg cytosol for the times shown, with or without Ac-DEVD-CHO or the caspase 3 and 7 inhibitor, Casputin™. Two cleavage products, C_1 and C_2, are indicated. Note that appearance of C_1 is prevented by Casputin™ and does not occur using CD-IC ($DSGA^{99}$). (B–D) Immunoprecipitated [^{35}S]methionine-labeled wild-type or mutated ($DSGA^{99}$) CD-IC was incubated for 2 h at 30°C with recombinant caspases 2 (B), 3 (C), and 7 (D). Caspase 2 activity was confirmed by assessing cleavage of in vitro–translated caspase 2, whilst caspases 3 and 7 were tested using in vitro–translated PARP. (E) Native *Xenopus* egg cytoplasmic dynein–dynactin was incubated with recombinant caspase 2 (50 nM) or caspase 3 (20 nM), ± Ac-DEVD-CHO for 3 h at 37°C. Proteins were analyzed after SDS-PAGE by immunoblotting (CD-IC was detected using polyclonal antiserum).

Biochemical Analysis of the Cytoplasmic Dynein and Dynactin Complexes during Apoptosis

Cytoplasmic dynein and dynactin sediment as separate complexes of ~20S. To test if caspase cleavage of CD-IC and p150^{Glued} affected the stability of the complexes, we compared their sedimentation properties when isolated from control and apoptotic egg cytosol. Motors bind statically to microtubules in the absence of ATP, so cytoplasmic dynein can be enriched from cytosol relatively simply. Dynactin copurifies with cytoplasmic dynein, since the p150^{Glued} subunit also possesses a microtubule binding domain (between amino acids 39–150; Waterman-Storer et al., 1995). Silver staining and immunoblotting of sucrose gradients of cytoplasmic dynein–dynactin-enriched fractions from control egg cytosol revealed that CD-HC, CD-IC, and CD-LIC cosedimented at 20S (in fractions 5 and 6; Fig. 5 A). In fractions enriched from apoptotic cytosol, CD-HC and CD-LIC were still found at 20S, even though full-length CD-IC could not be detected using 70.1 (Fig. 5 A). Hence, cleavage of CD-IC does not appear to destabilize CD-HC and CD-LIC interactions.

We next asked whether the large COOH-terminal CD-IC fragment also remained in the complex using an immunoprecipitation approach (Fig. 5, B and C). In many apoptotic egg extracts, cleavage of CD-IC is only ~60–70% efficient (Fig. 5 B, lanes 1 and 2). When we immunoprecipitated using anti–CD-LIC antibodies, we found that the CD-IC cleavage product, intact CD-IC (Fig. 5 B, lane 4), and CD-HC (not shown) coprecipitated efficiently. We wanted to know whether dynein complexes existed which only contained the cleaved CD-IC, and to address this we first depleted dynein containing intact CD-IC by three rounds of immunoprecipitation with an NH_2-terminal monoclonal antibody (1618), which does not recognize cleaved CD-IC (Fig. 5 C). Interestingly, cleaved CD-IC did not coprecipitate with intact CD-IC (Fig. 5 C, lanes 3–6), but remained in the unbound fraction (Fig. 5 C, lanes 7 and 8). Moreover, when we used anti–CD-LIC beads to immunoprecipitate the remaining dynein from full-length CD-IC–depleted apoptotic cytosol, the immune complexes contained the cleaved form of CD-IC along with CD-HC (Fig. 5 C, lane 10). These experiments suggest that, in *Xenopus* egg cytosol, cleavage of CD-IC chains does not cause the dynein components to disassociate. Strikingly, the dynein complexes contain either all intact or all cleaved CD-ICs.

Sucrose density gradient analysis also provided information on the dynactin complex. Using the monoclonal anti-p150^{Glued} antibody, we found that in control cytosol p150^{Glued} sedimented at 20S as expected (Fig. 5 A). In apoptotic cytosol, we detected some full-length p150^{Glued} at 20S (Fig. 5 A), since cleavage of p150^{Glued} is incomplete (Fig. 1 C). Although some cleaved p150^{Glued} also migrated to this position (Fig. 5 A), the majority was detected at the top of the gradient, suggesting that it had dissociated from the dynactin complex (Fig. 5 A). The method for isolating cleaved (and intact) p150^{Glued} relies on microtubule affinity, suggesting that the truncated product contains a functional microtubule binding domain (although some may be complexed with the small amount of intact, free p150^{Glued}). Moreover, the monoclonal p150^{Glued} antibody used was raised against the NH_2-terminal microtubule binding domain of p150^{Glued}, so it seems likely that the caspase cleavage site(s) within *Xenopus* p150^{Glued} is located towards its COOH terminus.

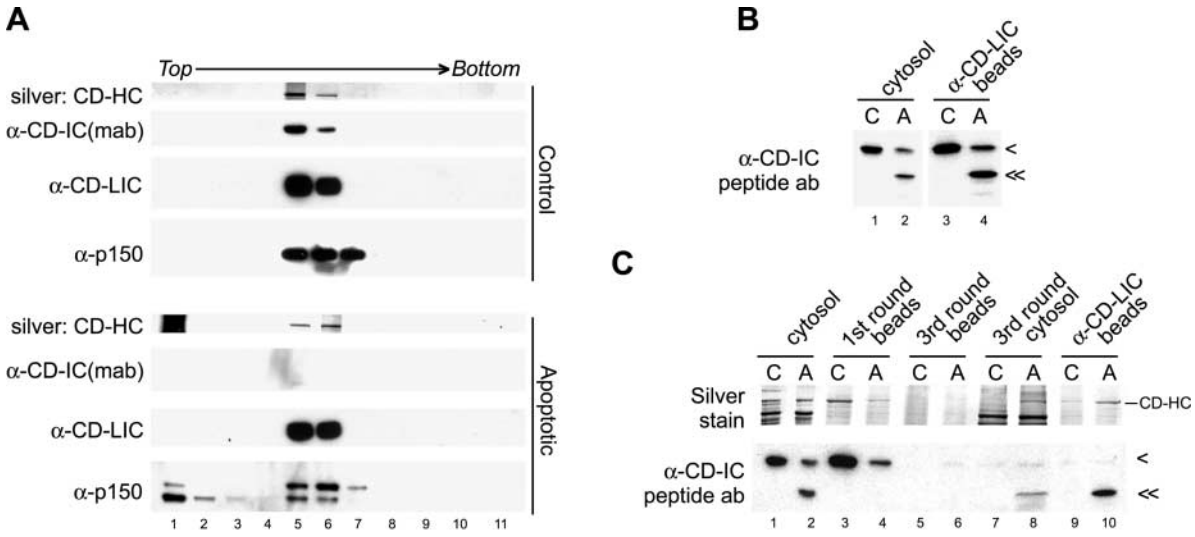

Figure 5. The fate of cytoplasmic dynein and dynactin complexes in apoptotic extracts. (A) Microtubule motors were isolated from control or apoptotic *Xenopus* egg cytosol by microtubule affinity, then separated on sucrose density gradients and analyzed by silver staining and immunoblotting (CD-IC was detected using 70.1). CD-HC was not seen in fraction 1 of the apoptotic gradient: the silver staining in that lane is artefactual. (B) The cytoplasmic dynein complex was immunoprecipitated from control (C) and apoptotic (A) egg cytosols using anti–CD-LIC antibody, and immunoblotted with polyclonal anti–CD-IC peptide antibody to detect cleaved (<<) and intact (<) CD-IC. (C) Control (C; lane 1) and apoptotic (A; lane 2) egg cytosols were depleted of any cytoplasmic dynein complex containing uncleaved CD-IC by three rounds of depletion using the monoclonal antibody, 1618, against the NH_2-terminus of CD-IC (beads from only rounds 1 and 3 are shown; lanes 3–6). The depleted cytosols (lanes 7 and 8) were then subjected to a further immunoprecipitation with anti–CD-LIC beads (lanes 9 and 10). All fractions were examined by silver stain for DHC (top) and immunoblotted with anti–CD-IC peptide antibody to detect cleaved (<<) and uncleaved (<) CD-IC (bottom).

Cleavage of CD-IC and p150^{Glued} Stops Cytoplasmic Dynein–driven Membrane Motility In Vitro

According to current models, caspase-mediated cleavage of CD-IC and p150^{Glued} should uncouple cytoplasmic dynein from its cargo and therefore prevent movement along microtubules. We tested this hypothesis using two approaches. First, we determined whether cytoplasmic dynein and dynactin remained membrane-associated in egg extracts during apoptosis, and then we looked at the consequences of apoptotic CD-IC and p150^{Glued} cleavage on membrane motility using an in vitro assay. Floated *Xenopus* egg membranes are rich in both cytoplasmic dynein and dynactin (Fig. 6; Lane and Allan, 1999). Although silver staining revealed very little difference in the overall protein pattern in apoptotic versus control cytosol or membranes (Fig. 6 A), the apoptotic membranes had lost most of their associated CD-LIC and CD-IC (Fig. 6 B). Since the cytoplasmic dynein complex remains intact during apoptosis (Fig. 5), it is likely that the entire complex is removed from membranes during this process.

We then looked at the dynactin complex. The amount of full-length and cleaved p150^{Glued} on apoptotic membranes was greatly reduced, and p50 dynamitin also appeared to be depleted (Fig. 6 B). Membrane-associated Arp-1 was partially degraded to an ~32-kD product in apoptotic egg extracts, which remained associated with membranes (no degradation was observed in apoptotic cytosol; Fig. 6 B). We do not know if the Arp-1 degradation product is due solely to the action of caspases, because we always observed a similar band in immunoblots of control membranes (Fig. 6 B). Taken together, these results suggest that at least part of the dynactin complex stays on apoptotic membranes. We also compared KHC and kinesin II on control and apoptotic membranes (Fig. 6 B). Interestingly, while the amounts of kinesin II (p85 subunit) did not change, we found that KHC, although uncleaved (Figs. 1 A and 6 B), was lost from apoptotic egg membranes, an observation which merits further investigation.

ER membranes present in crude frog egg extracts move exclusively using cytoplasmic dynein in egg cytosol and are easily identified by VE-DIC microscopy (Allan, 1995; Niclas et al., 1996; Lane and Allan, 1999). Therefore, we used in vitro motility assays to assess cytoplasmic dynein–based membrane motility in control and apoptotic egg extracts. Extensive ER networks formed from membranes and cytosol derived from control extracts treated with cytochrome *c* and caspase inhibitors (Fig. 7 A, left). The motility of these networks was identical to that seen in untreated extracts. However, upon combining membranes and cytosol from apoptotic extracts, we saw no network formation (Fig. 7 A, right). Instead, membrane clumps rarely associated with microtubules (Fig. 7 A), and tubule extension events were never observed. We have not assessed whether ER membrane fusion is also inhibited, but this is a possibility given that homotypic endosome fusion is a target for apoptotic regulation (via caspase 3 cleavage of Rabaptin 5; Cosulich et al., 1997; Swanton et al., 1999a).

These data suggest that apoptotic membranes are unable to form networks in apoptotic cytosol because they have lost the capacity to associate with and move along microtubules in a cytoplasmic dynein–dependent fashion. However, when apoptotic membranes were incubated in control cytosol, they regained the ability to move along microtubules and undergo homotypic membrane fusion (Fig. 7 B, left), generating networks which were ~75% as extensive as seen in nonapoptotic conditions. When we carried out the reciprocal experiment (control membranes in apoptotic cytosol), we found that the extent of network formation was similar (Fig. 7 B, right). All experiments were performed in the presence of caspase inhibitor to prevent further caspase action.

When the membranes from these incubations were reisolated and immunoblotted for cytoplasmic dynein and dynactin, we found that apoptotic membranes effectively recruited full-length CD-IC and CD-LIC, as well as p150^{Glued}, to ~50% of control levels in just 1 h (Fig. 8), although under identical conditions KHC was not recruited (data not shown). Control membranes lost a proportion of

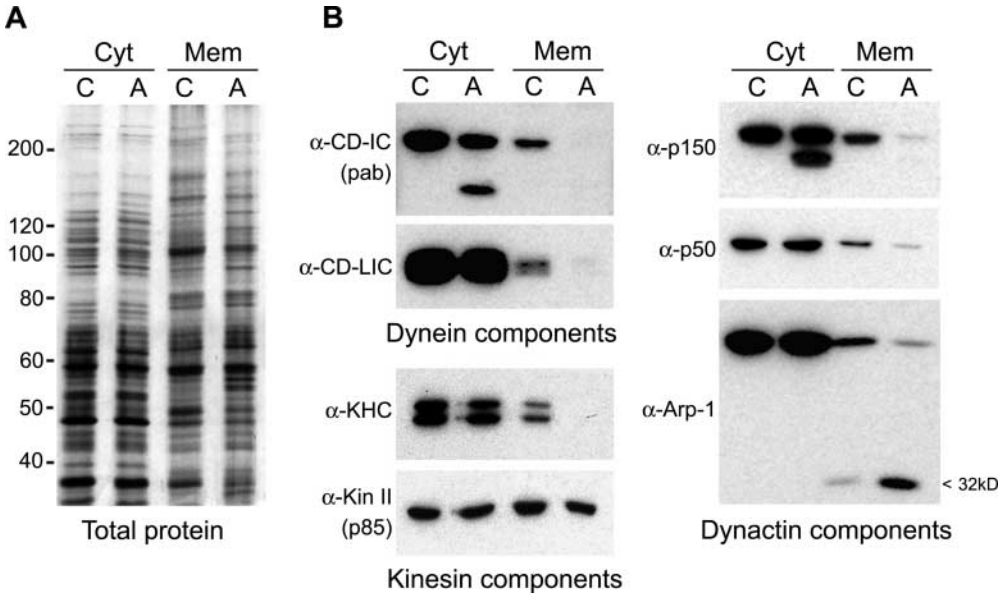

Figure 6. The cytoplasmic dynein complex is released from membranes during apoptosis in *Xenopus* egg extracts. Cytosol (Cyt) and membranes (Mem) were prepared from control or apoptotic extracts (C and A, respectively). Equal amounts of protein were loaded on SDS-PAGE gels, silver stained for total protein (A) and immunoblotted using the antibodies shown (B).

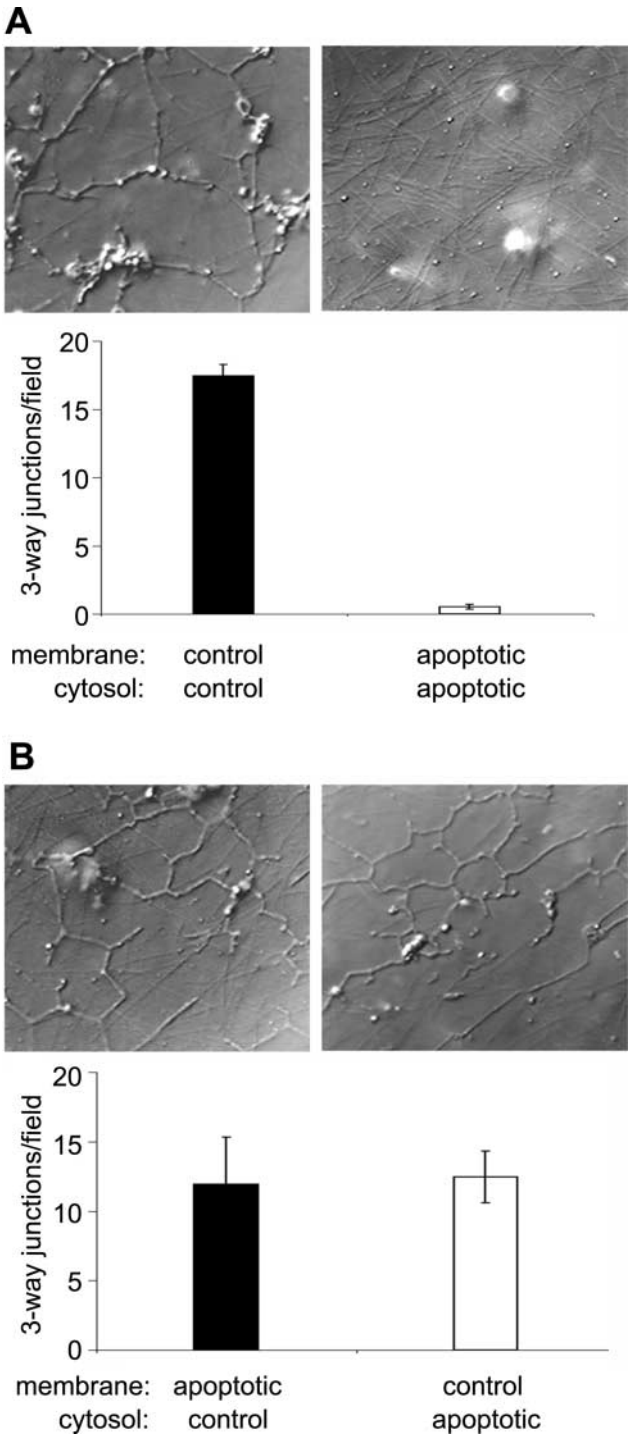

Figure 7. Motile properties of apoptotic and nonapoptotic membranes. (A) Membranes were prepared by flotation from control and apoptotic *Xenopus* egg extracts, then incubated in their respective cytosols for 45 min. They were then assayed for motility using a three way junction index (see Materials and Methods). (B) Control or apoptotic cytosols and membranes were mixed as indicated, and assayed for motility as above. Values are means ± SEM for three independent experiments. In each case, Ac-DEVD-CHO was added to a final concentration of 2 μM before motility assays. Representative VE-DIC fields (27 μm across) are also shown for each assay.

their associated cytoplasmic dynein and dynactin when incubated in apoptotic cytosol for 1 h (Fig. 8). This probably reflects the dynamic nature of cytoplasmic dynein's affinity for membranes and is not due to caspase activity, because Ac-DEVD-CHO was included in these assays.

We next asked whether membrane movement in apoptotic extracts could be restored by the addition of purified cytoplasmic dynein–dynactin. We incubated apoptotic membranes and cytosol (plus Ac-DEVD-CHO) in the presence of pig brain cytoplasmic dynein–dynactin (Fig. 9). This fraction restored the network-forming ability of apoptotic membranes to ~25% of control activity (Fig. 9 A). The addition of pig brain cytoplasmic dynein brought the amount of intact CD-IC present in the cytosol/membrane mixture to approximately control levels (Fig. 9 B). These results suggest that cytoplasmic dynein–driven ER motility is halted during apoptosis primarily through caspase-mediated cleavage of cytoplasmic dynein and dynactin components.

Discussion

We have investigated the fate of cytoplasmic dynein during apoptosis, both in vivo and in vitro, as part of an ongoing study into alterations in membrane traffic and cellular organization. We have used *Xenopus* egg extracts as a well-characterized model system, as they support regulated cytoplasmic dynein–driven ER movement (Allan, 1995; Niclas et al., 1996; Lane and Allan, 1999) and can be driven into apoptosis by the addition of cytochrome *c* (Kluck et al., 1997).

We have identified CD-IC as a target for caspase-dependent cleavage both in vivo and in cell-free extracts, and have demonstrated by site-directed mutagenesis and the use of specific antibodies that cleavage results in the loss of the NH_2-terminal p150^{Glued}-binding domain. In contrast, CD-HC and CD-LIC are unaffected and remain as a complex containing the COOH-terminal cleavage product of CD-IC. Interestingly, we found that dynein complexes either contained only full length or only cleaved CD-IC, suggesting that once a dynein molecule is targeted by the caspase (probably caspase 3), all the CD-IC chains are cleaved.

The p150^{Glued} component of dynactin is also cleaved, and most of the cleaved form no longer migrates as part of the 20S dynactin complex on sucrose density gradients. Since cleaved p150^{Glued} seems to maintain its ability to bind to microtubules and is still recognized by an antibody to its NH_2-terminal domain, it is likely that the cleavage occurs in its COOH-terminal domain, through which it interacts with the rest of the dynactin complex (Waterman-Storer et al., 1995). This behavior is remarkably similar to that of the COOH-terminally truncated product of the dominant *Glued*^{1} mutant gene in *Drosophila* (McGrail et al., 1995). It will clearly be of interest to map the p150^{Glued} cleavage site in future studies. Since some dynamitin and Arp1 stay bound to the membrane, this may mean that the dynactin complex minus p150^{Glued} is left behind. However, lack of antibodies recognizing other *Xenopus* dynactin components has prevented a thorough investigation of this question.

The cleavage of these two key components, CD-IC and p150^{Glued}, would be predicted to destroy cytoplasmic dynein's ability to bind to and therefore move cargo (Fig. 10),

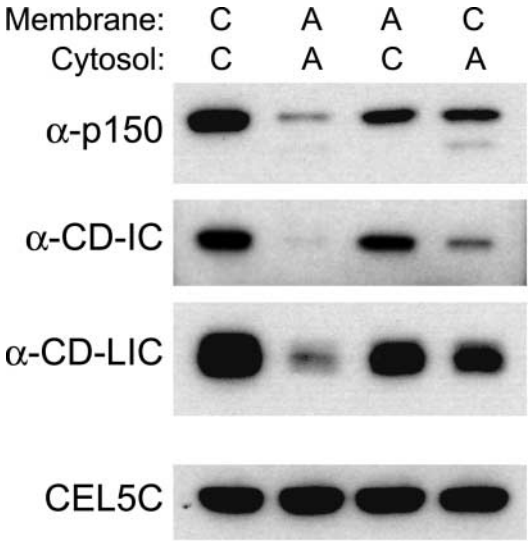

Figure 8. Apoptotic membranes can recruit intact cytoplasmic dynein and dynactin. Membranes from control (C) or apoptotic (A) egg extracts were incubated in control or apoptotic cytosol for 1 h. Membranes were then recovered and equal protein samples were run on SDS-PAGE and immunoblotted (antiribophorin was used as a loading control).

and we have shown this to be the case for cytoplasmic dynein–driven ER motility in apoptotic *Xenopus* egg extracts. Interestingly, apoptotic membranes recruit intact cytoplasmic dynein and dynactin from control cytoplasm, and regain the ability to form ER networks. Moreover, the addition of a pig brain cytoplasmic dynein fraction (which also contains dynactin) to a mixture of apoptotic cytosol and membranes was sufficient to reconstitute network formation partially. Although the amount of pig brain dynein added matched that present in control cytosol, motility was not fully restored. There are many possible explanations for this: first, we do not know how much of this dynein is recruited to the membrane; second, the purified dynein fraction may be partially inactive, or take time to become activated when added to cytosol; third, the concentration of dynactin may be too low; and fourth, there may be other factors that are absent in apoptotic cytosol that are required to restore full motility. Together, however, our data suggest that cytoplasmic dynein and dynactin are primary targets for the caspase-dependent abrogation of ER tubule movement described here. Any cleavage of integral membrane proteins by caspases cannot be inhibiting cytoplasmic dynein binding in our assay, as such changes would not be reversible.

Our results clearly demonstrate that the interaction of cytoplasmic dynein and dynactin with the membrane is dynamic, and suggests that there is rapid turnover, at least in the presence of apoptotic cytosol. This is in keeping with other studies in *Xenopus*, which have revealed that both cytoplasmic dynein and dynactin are rapidly released from membranes on entry into metaphase (Niclas et al., 1996; Addinall et al., 2001), or when anti–CD-IC antibodies are added to interphase extracts (Steffen et al., 1997). Similar loss of cytoplasmic dynein from membranes occurred after the addition of anti-p150^{Glued} antibodies to squid axoplasm (Waterman-Storer et al., 1997) and under certain conditions in cultured mammalian cells (Lin et al., 1994). In addition, overexpression of the dynamitin subunit of dynactin causes loss of cytoplasmic dynein from kinetochores (Echeverri et al., 1996) and the Golgi apparatus (Roghi and Allan, 1999), again demonstrating that cytoplasmic dynein–cargo interaction is dynamic.

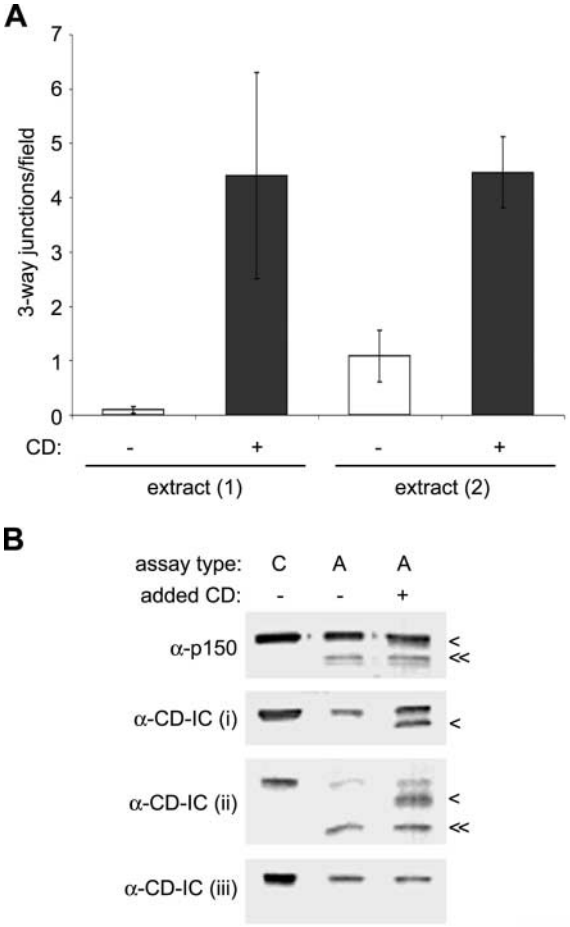

Figure 9. Addition of purified pig brain cytoplasmic dynein–dynactin restores ER network formation. (A) Membranes were prepared by flotation from apoptotic egg extracts, and incubated for 45 min in apoptotic cytosol in the presence or absence of pig brain cytoplasmic dynein–dynactin (CD). To avoid apoptotic cleavage of the added motor components, 2 μM Ac-DEVD-CHO was included in the motility assays. Values are means ± SEM for three independent experiments. (B) Total samples from a pig brain dynein–dynactin add-back experiment were immunoblotted using the antibodies shown (C, control cytosol and membranes; A, apoptotic cytosol and membranes). Anti–CD-IC antibodies: i, 70.1; ii, anti-*Xenopus* CD-IC peptide antibody; iii, *Xenopus*-specific NH_2-terminal antibody. The position of the added pig brain motor components (◀) and the *Xenopus* p150^{Glued} and CD-IC cleavage products (3) are shown. In contrast to Fig. 8, total samples, not re-isolated membranes, were analyzed.

What is the significance of these cleavage events to the apoptosing cell? As yet, we can only speculate, but it is clear that CD-IC in particular is an early target for cleavage, which proceeds in parallel with PARP cleavage. Given that inhibition of cytoplasmic dynein function disrupts ER-to-Golgi apparatus traffic (Presley et al., 1997) and leads to a scattering of the Golgi apparatus through-

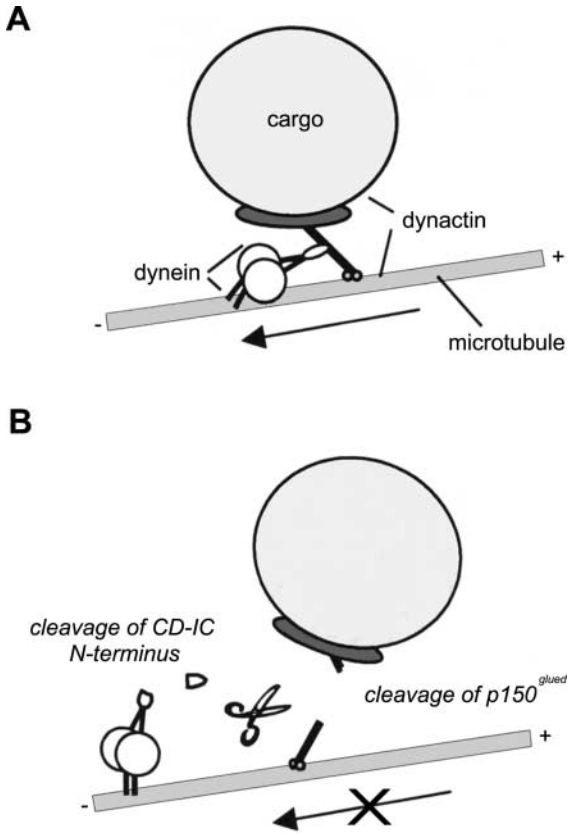

Figure 10. Diagram showing the predicted effects of CD-IC and p150^{Glued} cleavage on cytoplasmic dynein–driven organelle motility. Cleavage leads to the removal of the p150^{Glued}-binding domain of CD-IC, rendering cytoplasmic dynein incapable of binding to, and hence moving, its cargoes. Cleavage of p150^{Glued}, which occurs more slowly, removes the microtubule-binding capacity of the dynactin complex, which may ensure that cargoes cannot associate with microtubules. Our results suggest that p50 dynamitin is also partially released from cargo (not shown in model).

out the cell (Burkhardt et al., 1997; Quintyne et al., 1999; Roghi and Allan, 1999), it is intriguing to note that Golgi apparatus fragmentation is seen in apoptotic cells (Mancini et al., 2000). It will be of great interest to know if the loss of cytoplasmic dynein from the Golgi apparatus contributes to this phenotype, and whether ER-to-Golgi apparatus traffic is also inhibited due to a lack of motor.

In this study, we have investigated the effects of apoptosis on membrane movement, but since cytoplasmic dynein plays many different roles in the cell, it is plausible that interrupting other cytoplasmic dynein–driven motile events may also be important for apoptosis. Another issue is that the cleavage site that we have identified in *Xenopus* CD-IC, DSGD^{99}G, is conserved in all rat CD-IC2 splice forms but not in rat CD-IC1. The cytoplasmic dynein intermediate chain family is encoded by two genes, of which CD-IC1 is expressed only in brain and testis, while CD-IC2 is found in all tissues (for review see Susalka et al., 2000). Therefore, all cells are likely to contain a cleavable CD-IC, while neurons and testis may also possess a form that lacks this caspase cleavage site. This may provide a means of differentially regulating the function of distinct cytoplasmic dynein complexes during apoptosis.

Cytoplasmic dynein has been proposed to play a direct role in an early, caspase-independent signaling event during apoptosis. The cytoplasmic dynein light chain, LC8, and the proapoptotic protein Bim (O'Connor et al., 1998) are stably associated with each other in healthy cells, and translocate to Bcl-2 shortly after triggering apoptosis (Pakthalakath et al., 1999). Hence, caspase-dependent inactivation of the cytoplasmic dynein–dynactin complex might provide a positive feed-back loop during activation of the apoptotic cascade. However, LC8 is also a component of flagellar dynein, myosin V, IκBα and nitric oxide synthase (for review see King, 2000). In addition, the expression of LC8 is increased by cyclooxygenase 2 treatment of PC12 cells, where it is thought to protect from growth factor withdrawal-induced apoptosis by the inhibition of nitric oxide synthesis (Chang et al., 2000). Therefore, because of the apparent promiscuous behavior of LC8, and in the absence of definitive evidence that Bim is part of the native cytoplasmic dynein complex, it remains unclear whether the cleavage of CD-IC that we observe here will have any direct effects on the Bim-LC8 interaction.

Little else is known about the roles that microtubule motors play in apoptosis. An inhibition of the plus end–directed microtubule motor, kinesin, has been implicated in the clustering of mitochondria that occurs on triggering cell death via tumor necrosis factor (De Vos et al., 1998, 2000), but as a shift in mitochondrial position did not occur after other apoptotic stimuli, it is not clear if this is a general phenomenon. Whether inactivation of kinesin is also responsible for Bax-induced mitochondrial clustering (Desagher and Martinou, 2000) remains to be tested. Interestingly, our results show that kinesin, like dynein, was released from apoptotic membranes (Fig. 6), but it was not rerecruited from control cytosol (data not shown). Although KHC is not cleaved in apoptotic egg extracts, we do not yet know if kinesin light chains, which are thought to target kinesin to its cargoes (Hollenbeck, 2001), are affected. In addition, since caspase-induced cleavage of kinectin has been seen in apoptotic cultured cells (Machleidt et al., 1998), this raises the possibility that kinectin is also cleaved on apoptotic membranes in our assay system, and that this prevents rerecruitment.

The identification of cytoplasmic dynein and dynactin as targets for degradation adds to the list of key cytoskeletal (Brancolini et al., 1995; Caulín et al., 1997; Mills et al., 1999) and trafficking molecules (Cosulich et al., 1997; Swanton et al., 1999a; Mancini et al., 2000) that are cleaved during the crucial process of apoptosis. A key issue will be to understand how these changes together expedite the recognition and clearance of apoptotic cells.

We thank Birgit Lane, David Meyer, Jon Scholey, Ron Vale, and Richard Vallee for supplying antibodies, and Don Nicholson and Sophie Roy for caspases. We are grateful to Martin Lowe and Lisa Swanton for comments and advice.

This work was supported by the Biotechnology and Biological Sciences Research Council (34/BI11195 to V. Allan and P. Woodman), the Lister Institute for Preventive Medicine (V. Allan) and the Medical Research Council (G117/153 to P. Woodman; and COG grant G9722026).

Submitted: 9 November 2000
Revised: 10 May 2001
Accepted: 15 May 2001

References

Addinall, S., P. Mayr, S. Doyle, J. Sheehan, P. Woodman, and V. Allan. 2001. Phosphorylation by cdc2-cyclinB1 kinase releases cytoplasmic dynein from membranes. *J. Biol. Chem.* 276:15939–15944.

Allan, V. 1995. Protein phosphatase 1 regulates the cytoplasmic dynein-driven formation of endoplasmic reticulum networks in vitro. *J. Cell Biol.* 128:879–891.

Allan, V. 1996. Motor proteins: a dynamic duo. *Curr. Biol.* 6:630–633.

Allan, V.J. 1998. Organelle motility and membrane network formation in metaphase and interphase cell-free extracts. *Methods Enzymol.* 298:339–353.

Allan, V.J., and R.D. Vale. 1991. Cell cycle control of microtubule-based membrane transport and tubule formation in vitro. *J. Cell Biol.* 113:347–359.

Balch, W.E., W.G. Dunphy, W.A. Braell, and J.E. Rothman. 1984. Reconstitution of the transport of protein between successive compartments of the Golgi measured by the coupled incorporation of N-acetylglucosamine. *Cell*. 39:405–416.

Blocker, A., F. Severin, J. Burkhardt, J. Bingham, H. Yu, J.-C. Olivo, T. Schroer, A. Hyman, and G. Griffiths. 1997. Molecular requirements for bi-directional movement of phagosomes along microtubules. *J. Cell Biol.* 137: 113–129.

Brancolini, C., M. Benedetti, and C. Schneider. 1995. Microfilament reorganization during apoptosis: the role of Gas2, a possible substrate for ICE-like proteases. *EMBO J*. 14:5179–5190.

Burkhardt, J., C. Echeverri, T. Nilsson, and R. Vallee. 1997. Overexpression of the dynamitin (p50) subunit of the dynactin complex disrupts dynein-dependent maintenance of membrane organelle distribution. *J. Cell Biol.* 139:469–484.

Caulín, C., G. Salvesen, and R. Oshima. 1997. Caspase cleavage of keratin 18 and reorganization of intermediate filaments during epithelial cell apoptosis. *J. Cell Biol.* 138:1379–1394.

Chang, Y.-W.E., R. Jakobi, A. McGinty, M. Foshi, M.J. Dunn, and A. Sorokin. 2000. Cyclooxygenase 2 promotes cell survival by stimulation of dynein light chain expression and inhibition of neuronal nitric oxide synthase activity. *Mol. Cell. Biol.* 20:8571–8579.

Cohen, G.M. 1997. Caspases: the executioners of apoptosis. *Biochem. J.* 326:1–16.

Cosulich, S., S. Green, and P. Clarke. 1996. Bcl-2 regulates activation of apoptotic proteases in a cell-free system. *Curr. Biol.* 6:997–1995.

Cosulich, A., H. Horiuchi, M. Zerial, P. Clarke, and P. Woodman. 1997. Cleavage of rabaptin-5 blocks endosome fusion during apoptosis. *EMBO J.* 16: 6182–6191.

Desagher, S., and J.-C. Martinou. 2000. Mitochondria as the central control point of apoptosis. *Trends Cell Biol.* 10:369–377.

Devitt, A., O.D. Moffatt, C. Raykundalia, J.D. Capra, D.L. Simmons, and C.D. Gregory. 1998. Human CD14 mediates recognition and phagocytosis of apoptotic cells. *Nature*. 392:442–443.

De Vos, K., V. Goossens, E. Boone, D. Vercammen, K. Vancompernolle, P. Vandenabeele, G. Haegeman, W. Fiers, and J. Grooten. 1998. The 55-kDa tumor necrosis factor receptor induces clustering of mitochondria through its membrane-proximal region. *J. Biol. Chem.* 273:9673–9680.

De Vos, K., F. Severin, F. Van Herreweghe, K. Vancompernolle, V. Goossens, A. Hyman, and J. Grooten. 2000. Tumor necrosis factor induces hyperphosphorylation of kinesin light chain and inhibits kinesin-mediated transport of mitochondria. *J. Cell Biol.* 149:1207–1214.

Echeverri, C.J., B.M. Paschal, K.T. Vaughan, and R.B. Vallee. 1996. Molecular characterisation of the 50-kD subunit of dynactin reveals function for the complex in chromosome alignment and spindle organization during mitosis. *J. Cell Biol.* 132:617–633.

Fadok, V.A., D.L. Bratton, D.M. Rose, A. Pearson, R.A. Ezekewitz, and P.M. Henson. 2000. A receptor for phosphatidylserine-specific clearance of apoptotic cells. *Nature*. 405:85–90.

Gill, S.R., T.A. Schroer, I. Szilak, E.R. Steuer, and M.P. Sheetz. 1991. Dynactin, a conserved, ubiquitously expressed component of an activator of vesicle motility mediated by cytoplasmic dynein. *J. Cell Biol.* 115:1639–1650.

Hamon, Y., C. Broccardo, O. Chambenoit, M.-F. Luciani, F. Toti, S. Chaslin, J.-M. Freyssinet, P.F. Devaux, J. McNeish, D. Marguet, and G. Chimini. 2000. ABC1 promotes engulfment of apoptotic cells and transbilayer redistribution of phosphatidylserine. *Nat. Cell Biol.* 2:399–406.

Harada, A., Y. Takei, Y. Kanai, Y. Tanaka, S. Nonaka, and N. Hirokawa. 1998. Golgi vesiculation and lysosome dispersion in cells lacking cytoplasmic dynein. *J. Cell Biol.* 141:51–59.

Hollenbeck, P. 2001. Kinesin delivers: identifying receptors for motor proteins. *J. Cell Biol.* 152:F25–F27.

Karki, S., and E.L.F. Holzbaur. 1995. Affinity chromatography demonstrates a direct binding between cytoplasmic dynein and the dynactin complex. *J. Biol. Chem.* 270:28806–28811.

Karki, S., and E. Holzbaur. 1999. Cytoplasmic dynein and dynactin in cell division and intracellular transport. *Curr. Opin. Cell Biol.* 11:45–53.

King, S. 2000. The dynein microtubule motor. *Biochim. Biophys. Acta*. 1496:60–75.

King, S., and T. Schroer. 1999. Dynactin increases the processivity of the cytoplasmic dynein motor. *Nat. Cell Biol.* 2:20–24.

Kluck, R.M., S.J. Martin, B.M. Hoffman, J.S. Zhou, D.R. Green, and D.D. Newmeyer. 1997. Cytochrome c activation of CPP32-like proteolysis plays a critical role in a *Xenopus* cell-free apoptosis system. *EMBO J.* 16:4639–4649.

Lane, J.D., and V.J. Allan. 1999. Microtubule-based endoplasmic reticulum motility in *Xenopus laevis*: activation of membrane-associated kinesin during development. *Mol. Biol. Cell*. 10:1909–1922.

Lin, S.X., K.L. Ferro, and C.A. Collins. 1994. Cytoplasmic dynein undergoes intracellular redistribution concomitant with phosphorylation of the heavy chain in response to serum starvation and okadaic acid. *J. Cell Biol.* 127: 1009–1019.

Liu, X., C.N. Kim, J. Yang, R. Jemmerson, and X. Wang. 1996. Induction of apoptotic program in cell-free extracts: requirement for dATP and cytochrome c. *Cell*. 86:147–158.

Machleidt, T., P. Geller, R. Schwander, G. Scherer, and M. Krönke. 1998. Caspase-7 induced cleavage of kinectin in apoptotic cells. *FEBS Lett.* 436:51–54.

Mancini, M., C. Machamer, S. Roy, D. Nicholson, N. Thornberry, L. Casciola-Rosen, and A. Rosen. 2000. Caspase-2 is localized at the Golgi complex and cleaves Golgin-160 during apoptosis. *J. Cell Biol.* 149:603–612.

Martin, S.J., C.P.M. Reutelingsperger, A.J. McGahon, J.A. Rader, R.C.A.A. van Schie, D.M. LaFace, and D.R. Green. 1995. Early redistribution of plasma membrane phosphatidylserine is a general feature of apoptosis regardless of the initiating stimulus: inhibition by overexpression of Bcl-2 and Abl. *J. Exp. Med.* 182:1545–1556.

McGrail, M., J. Gepner, A. Silvanovich, S. Ludmann, M. Serr, and T.S. Hays. 1995. Regulation of cytoplasmic dynein function in vivo by the *Drosophila Glued* complex. *J. Cell Biol.* 131:411–425.

Mills, J., N. Stone, and R. Pittman. 1999. Extranuclear apoptosis: the role of the cytoplasm in the execution phase. *J. Cell Biol.* 146:703–707.

Muresan, V., M. Stankewich, W. Steffen, J. Morrow, E. Holzbaur, and B. Schnapp. 2001. Dynactin-dependent, dynein-driven vesicle transport in the absence of membrane proteins: a role for spectrin and acidic phospholipids. *Mol. Cell*. 7:173–183.

Murray, A. 1991. Cell cycle extracts. *Methods Cell Biol.* 36:581–605.

Newmeyer, D., D. Farschon, and J. Reed. 1994. Cell-free apoptosis in *Xenopus* egg extracts: inhibition by Bcl-2 and requirement for an organelle fraction enriched in mitochondria. *Cell*. 79:353–364.

Niclas, J., V.J. Allan, and R.D. Vale. 1996. Cell cycle regulation of dynein association with membranes modulates microtubule-based organelle transport. *J. Cell Biol.* 133:585–593.

Nicolás, F., C. Zhang, M. Hughes, M. Goldberg, S. Watton, and P. Clarke. 1997. *Xenopus* Ran-binding protein 1: molecular interactions and effects on nuclear assembly in *Xenopus* egg extracts. *J. Cell Sci.* 110:3019–3030.

O'Connor, L., A. Strasser, L.A. O'Reilly, G. Hausmann, J.M. Adams, S. Cory, and D.C.S. Huang. 1998. Bim: a novel member of the Bcl-2 family that promotes apoptosis. *EMBO J.* 17:384–395.

Pakthalakath, H., D. Huang, L. O'Reilly, S. King, and A. Strasser. 1999. The proapototic activity of the Bcl-2 family member Bim is regulated by interaction with the dynein motor complex. *Mol. Cell*. 3:287–296.

Parnaik, R., M.C. Raff, and J. Scholes. 2000. Differences between the clearance of apoptotic cells by professional and non-professional phagocytes. *Curr. Biol.* 10:857–860.

Platt, N., H. Suzuki, Y. Kurihara, T. Kodama, and S. Gordon. 1996. Role for the class A macrophage scavenger receptor in the phagocytosis of apoptotic thymocytes in vitro. *Proc. Natl. Acad. Sci. USA*. 93:12456–12460.

Presley, J.F., N.B. Cole, T.A. Schroer, K. Hirschberg, K.J.M. Zaal, and J. Lippincott-Schwartz. 1997. ER-to-Golgi transport visualized in living cells. *Nature*. 389:81–85.

Quintyne, N., S. Gill, D. Eckley, C. Crego, D. Compton, and T. Schroer. 1999. Dynactin is required for microtubule anchoring at centrosomes. *J. Cell Biol.* 147:321–334.

Ren, L., R.L. Silverstein, J. Allen, and J. Savill. 1995. CD36 gene transfer confers capacity for phagocytosis of cells undergoing apoptosis. *J. Exp. Med.* 181:1857–1862.

Roghi, C., and V. Allan. 1999. Dynamic association of cytoplasmic dynein heavy chain 1a with the Golgi apparatus and intermediate compartment. *J. Cell Sci.* 112:4673–4685.

Savill, J., I. Dransfield, N. Hogg, and C. Haslett. 1990. Vibronectin receptor-mediated phagocytosis of cells undergoing apoptosis. *Nature*. 343:170–173.

Schafer, D.A., S.R. Gill, J.A. Cooper, J.E. Heuser, and T.A. Schroer. 1994. Ultrastructural analysis of the dynactin complex: an actin-related protein is a component of a filament that resembles F-actin. *J. Cell Biol.* 126:403–412.

Schroer, T. 1996. Structure and function of dynactin. *Semin. Cell Dev. Biol.* 7:321–328.

Steffen, W., S. Karki, K.T. Vaughan, R.B. Vallee, E.L.F. Holzbaur, D.G. Weiss, and S.A. Kuznetsov. 1997. The involvement of the intermediate chain of cytoplasmic dynein in binding the motor complex to membranous organelles of *Xenopus* oocytes. *Mol. Biol. Cell*. 8:2077–2088.

Susalka, S., W. Hancock, and K. Pfister. 2000. Distinct cytoplasmic dynein complexes are transported by different mechanisms in axons. *Biochim. Biophys. Acta*. 1496:76–88.

Swanton, E., N. Bishop, and P.G. Woodman. 1999a. Human Rabaptin-5 is selectively cleaved by caspase-3 during apoptosis. *J. Biol. Chem.* 274:37583–37590.

Swanton, E., P. Savory, S. Cosulich, P. Clarke, and P. Woodman. 1999b. Bcl-2 regulates a caspase-3/caspase-2 apoptotic cascade in cytosolic extracts. *Oncogene*. 18:1781–1787.

Valetti, C., D. Wetzel, M. Schrader, M. Hasbani, S. Gill, T. Kreis, and T. Schroer. 1999. Role of dynactin in endocytic traffic: effects of dynamitin overexpression and colocalization with CLIP-170. *Mol. Biol. Cell.* 10:4107–4120.

Vaughan, K.T., and R.B. Vallee. 1995. Cytoplasmic dynein binds dynactin through a direct interaction between the intermediate chains and p150Glued. *J. Cell Biol.* 131:1507–1516.

Waterman-Storer, C.M., S. Karki, and E.L. Holzbaur. 1995. The p150Glued component of the dynactin complex binds to both microtubules and the actin-related protein centractin (Arp-1). *Proc. Natl. Acad. Sci. USA.* 92:1634–1638.

Waterman-Storer, C.M., S.B. Karki, S.A. Kuznetsov, J.S. Tabb, D.G. Weiss, G.M. Langford, and E.L.F. Holzbaur. 1997. The interaction between cytoplasmic dynein and dynactin is required for fast axonal transport. *Proc. Natl. Acad. Sci. USA.* 94:12180–12185.

Whyte, M., L. Meagher, J. MacDermot, and C. Haslett. 1993. Impairment of function in ageing neutrophils is associated with apoptosis. *J. Immunol.* 150: 5124–5134.

Wyllie, A.H., J.F.R. Kerr, and A.R. Currie. 1980. Cell death: the significance of apoptosis. *Int. Rev. Cytol.* 68:251–306.